ELSEVIER

Journal of Chromatography A, 857 (1999) 193–204

JOURNAL OF CHROMATOGRAPHY A

www.elsevier.com/locate/chroma

Magnetic split-flow thin fractionation of magnetically susceptible particles

C. Bor Fuh*, S.Y. Chen

Department of Applied Chemistry, Chaoyang University of Technology, 168 Gifeng East Road, Wufeng, Taichung County 413, Taiwan

Received 2 February 1999; received in revised form 10 May 1999; accepted 29 June 1999

Abstract

We recently built a magnetic separation system to extend the applications of split-flow thin (SPLITT) fractionation to magnetically susceptible particles. Here, we characterize the magnetic SPLITT system using magnetically susceptible particles and ion-labeled particles. The flow axis of separation channel was orientated parallel and perpendicular to gravitational forces to exclude and include, respectively, gravitational effects on separation. Both operating modes were used to test the theory experimentally, with emphasis on the parallel mode. The magnetic susceptibilities of carrier and ion-labeled particles were varied, and various ion-labeled and unlabeled particles were studied experimentally, resulting in successful separation of labeled particles, yeasts, and cells from unlabeled ones. The minimal difference in magnetic susceptibility ($\Delta\chi$) required for complete particle separation was about 1.75×10^{-5} [cgs], corresponding to about 10^9 labeling ions per particle in this study. The throughput was around 7.2×10^8 particles/h using the present setup. Magnetic SPLITT fractionation shows good potential for use in obtaining particles magnetic susceptibilities from a simple theoretical treatment.

Keywords: Split-flow thin fractionation; Magnetic separation

1. Introduction

Split-flow thin (SPLITT) fractionation has gradually become a very useful family for the separation of macromolecules, colloids and particles [1–10]. SPLITT fractionation has advantages for preparative separation of large molecules ($MW>10^6$) with throughput in the gram(s) or sub-g/h depending on the applying field [3,6,10]. SPLITT fractionation (SF) uses ribbon-like thin channels (<0.5 mm) and fields applied perpendicular to channel axis for separation. The channel is unpacked and the channel flow is parabolic. SPLITT channels are geometrically simple with one or more outlet splitters, that allow fractionated components to be collected without remixing. Fractionation of sample components at outlets can be calculated from the first principle when the transport parameters of samples and applied fields are known. SF theory provides good guidelines and predictions for experimental starting points and successful separation of samples with known physical properties and given applied fields. SF features include rapid separation process, continuous sample introduction, readily augmented throughput, relatively high resolution, and flexible separation process. The separation process speed is

*Corresponding author. Tel.: +886-4-332-3000; fax: +886-4-374-2341.

E-mail address: cbfuh@mail.cyut.edu.tw (C.B. Fuh)

0021-9673/99/$ – see front matter
PII: S0021-9673(99)00775-X

due to short separation distance (around 100 μm), and throughputs can readily be augmented by using higher field strengths and larger flow cell areas. The resolution is usually high (especially for particles) because flows are uniform in SPLITT channels, and no adverse effects are present. The flexible separation process comes from having adjustable flow-rates and field strengths. Currently, gravitational, centrifugal and electrical forces are used for SPLITT fractionation but adding other selection forces for separation is very important because of the increasingly challenging samples we must handle. Magnetic separations are rapid and selective, and those that use permanent magnet(s) have the additional benefits of economy and simplicity.

In an earlier paper we reported on assembly of a new magnetic SPLITT system and demonstrated its workability [12]. We introduced a new operating mode that used only magnetic force for separation in SPLITT system. We characterized the system in two modes using various particles and ion-labeled particles with magnetic susceptibility, emphasizing on the parallel mode since the perpendicular mode was emphasized in our earlier paper [12].

2. Theory

Experiments were done using perpendicular and parallel mode setups as shown in Figs. 1 and 2. In the perpendicular mode, the flow axis was orientated horizontally and perpendicular to gravity as shown in Fig. 1. In the parallel mode, the flow axis was orientated vertically and parallel to gravity to eliminate gravitational effects on separation, as shown in Fig. 2. Magnetic and gravitational forces were used for separation in the perpendicular mode, while only magnetic force was used for separation in the parallel mode. In the perpendicular mode, magnetic and gravitational forces were applied in opposite directions on the channel to facilitate separation [12]. Sample-free carriers were introduced into inlet a′ to confine the samples with carriers at inlet b′ into a small zone close to the bottom wall of the channel.

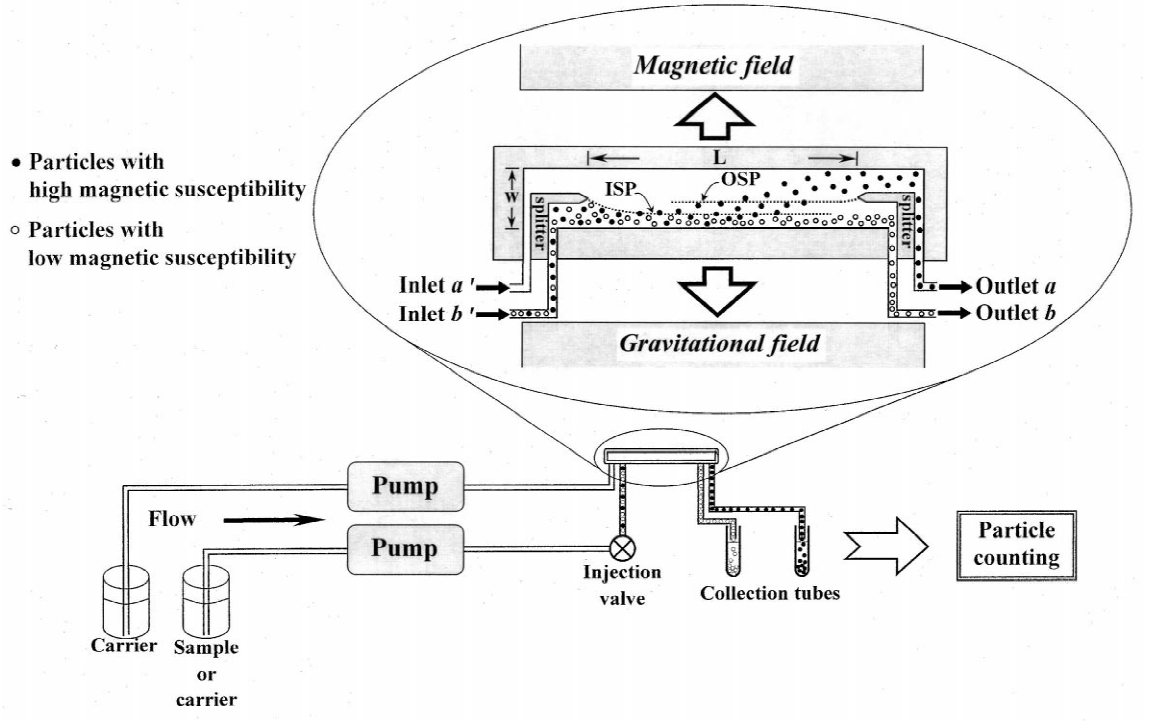

Fig. 1. Diagram of perpendicular magnetic SPLITT setup with flow axis horizontal and perpendicular to gravity. Magnetic force was applied upward and gravitational force acted downward. The flow-rate conditions were: $\dot{V}(a') > \dot{V}(b')$, $\dot{V}(a) = \dot{V}(b)$ and $\dot{V}(b) > \dot{V}(b')$.

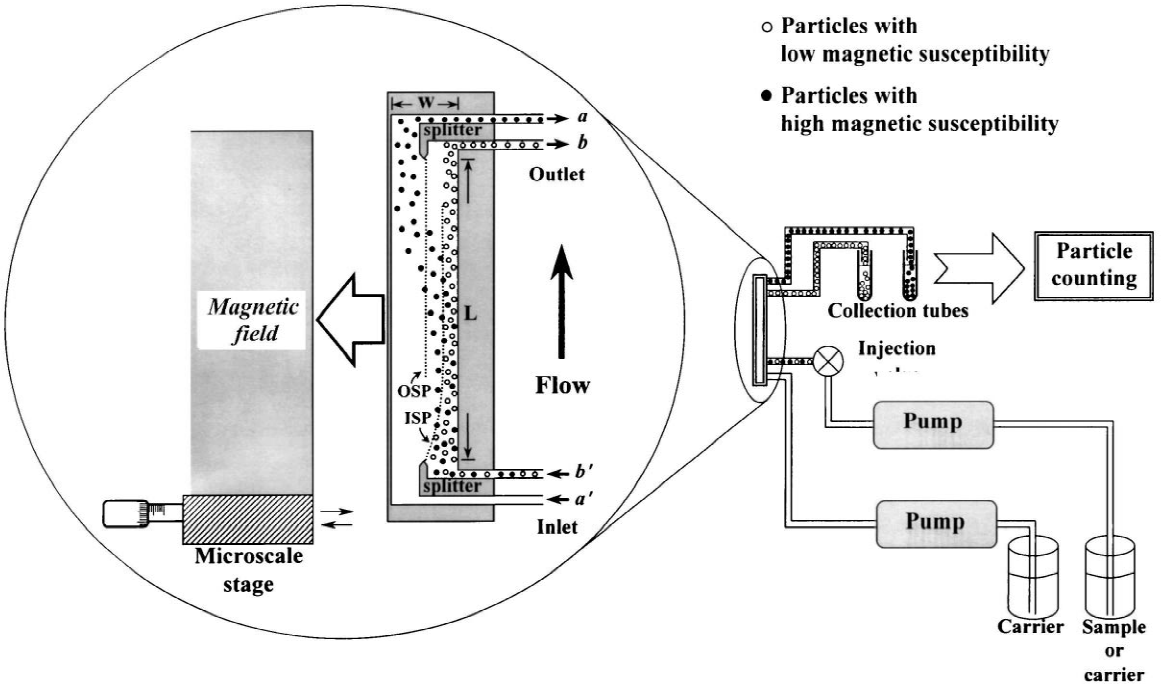

Fig. 2. Diagram of vertical magnetic SPLITT setup with flow axis vertical and parallel to gravity. Magnetic force was applied horizontally toward left. The flow-rate conditions were: $\dot{V}(a') > \dot{V}(b')$, $\dot{V}(a) = \dot{V}(b)$, and $\dot{V}(b) > \dot{V}(b')$.

Magnetic force drove the particles with high magnetic susceptibility (shown as solid circles in the figure) upward toward the top wall, while sample components passed along the channel below. Particles with low magnetic susceptibility (shown as hollow circles in the figure) settled toward the bottom wall due to gravitational force. Particles with high magnetic susceptibility tended to exit at outlet a, and particles with low magnetic susceptibility tended to exit at outlet b. In the parallel mode, magnetic force only drove the particles with high magnetic susceptibility (shown as solid circles in the figure) toward the left, while sample components passed along the right-hand side of the channel. Particles with high magnetic susceptibility tended to exit at outlet a, and particles with low magnetic susceptibility tended to exit at outlet b. Similarly, in the parallel mode, magnetic force alone drove the particles with high magnetic susceptibility toward the left and tended to force them to exit at outlet a, while particles with low magnetic susceptibility tended to exit at outlet b.

The theory behind system operation has been discussed elsewhere [3,8,12], thus need only briefly summarize the perpendicular-mode portion and then deduce the theory of parallel-mode operation. For a species to be transported across a lamina of flow-rate $\dot{V}i$, the magnetically induced flow-rate (bLU_m) must be larger than or equal to $\dot{V}i$, as shown in the following equation [2,12]:

$$bLU_m \geq \dot{V}i \quad (1)$$

where b is the channel breadth, L is the channel length, and U_m is the magnetically induced velocity.

Perpendicular-mode operation: All particles with high magnetic susceptibility exit at outlet a when Eq. (2) below is satisfied, which means that the net flow-rate resulting from subtracting the magnetically induced flow-rate (bLU_m) from the gravitationally induced flow-rate (bLU_g) is higher than the flow-rate at outlet b. Similarly, all particles with low magnetic susceptibilities exit at outlet b when Eq. (3) below is satisfied. The requirement that particles with very low magnetic susceptibility be fully retrieved at outlet b proceeds quite straightforwardly from Eq.

(3) when $\dot{V}(b) > \dot{V}(b')$ (i.e., the volumetric flow-rate at outlet b is higher than that at inlet b′). The flow-rate conditions used in this study kept $\dot{V}(b) > \dot{V}(b')$. In order to have complete separation, the following Eqs. (2) and (3) must both be satisfied for particles with, respectively, high and low magnetic susceptibilities [12]:

$$bLU_{mh} - bLU_g \geq \dot{V}(b) \tag{2}$$

$$bLU_{ml} - bLU_g < \dot{V}(b) - \dot{V}(b') \tag{3}$$

where U_m is the magnetically induced velocity (U_{mh} and U_{ml} are used for magnetically induced velocities of particles with high and low magnetic susceptibilities, respectively), U_g is the gravitationally induced velocity, $\dot{V}(b)$ is the volumetric flow-rate at outlet b, and $\dot{V}(b')$ is the volumetric flow-rate at inlet b′. Magnetically induced velocity, U_m, can be calculated using [12,13]:

$$U_m = \frac{\Delta\chi \Delta H^2 d}{48\eta} \tag{4}$$

where $\Delta\chi = \chi_p - \chi c$, χ_p and χ_c are the respective magnetic susceptibilities of particles and carriers, η is the fluid viscosity, d is the spherical particle diameter or the effective spherical diameter, and ΔH is the local magnetic field gradient. Gravitationally induced velocity, U_g, can be calculated using:

$$U_g = \frac{\Delta\rho d^2 g}{18\eta} \tag{5}$$

where η is the fluid viscosity, $\Delta\rho$ is the particle density minus the carrier fluid density, g is gravitational acceleration, and d is the spherical particle diameter or the effective spherical diameter. For particles with magnetically induced velocity, U_m is between U_{mh} and U_{ml} i.e., $\dot{V}(b) - \dot{V}(b') \leq bLU_m - bLU_g < \dot{V}(b)$, and the fraction of particles exiting at outlet a can be calculated using:

$$\frac{bLU_m - bLU_g - \dot{V}(b) + \dot{V}(b')}{\dot{V}(b')} \tag{6}$$

Parallel-mode operation: Gravity plays no role in this kind of separation since the flow axis is parallel to gravitational force. This means that the gravitationally induced flow-rate is zero in Eqs. (2), (3) and (6). It therefore follows straightforwardly that Eqs. (7) and (8) below must both be satisfied to have complete separation.

$$bLU_{mh} \geq \dot{V}(b) \tag{7}$$

$$bLU_{ml} < \dot{V}(b) - \dot{V}(b') \tag{8}$$

For particles with magnetically induced velocity, U_m is between U_{mh} and U_{ml}, i.e. $\dot{V}(b) - \dot{V}(b') \leq bLU_m < \dot{V}(b)$, and the fraction of particles exiting at outlet a can be calculated using:

$$\frac{bLU_m - \dot{V}(b) + \dot{V}(b')}{\dot{V}(b')} \tag{9}$$

3. Experimental

Two channel geometries were used in this study. Both channels were the same in length (10 cm) and breadth (0.5 cm), one was 0.025 cm thick and the other 0.010 cm thick. The injection loop had a volume of 0.5 ml when the system was used for testing and optimization. Channel components are shown in Fig. 3. The channels consisted of three layers of cut-out mylar with the ends of the center piece used as inlet and outlet splitters. All layers were then sandwiched together between sheets of plastic, which served as the channel walls.

Magnetic field was generated by a permanent magnet assembly consisting of one pair of rare earth magnets (Nd–Fe–B) [12]. The magnets were connected by soft iron pole pieces, which conducted the magnetic fluxes to the interpolar gap. The Nd–Fe–B (neodymium-iron-boron) magnets, characterized by maximum energy products of 3.0×10^7 Gauss-Oersteds were obtained from Super Electronics (Taipei, Taiwan), and were used for all experiments in this study. Magnetic field strengths were generated by gap widths of 5 mm and gap length of 10 cm for all experiments. Magnetic field measurements were made using a Gaussmeter and a Hall effect probe (Model Gauss MG-7D, Walker Scientific, Worcester, MA). The probe measured magnetic flux perpendicular to a sensing area with a diameter of 6.94 mm, and polar coordinates (r, θ) with (0, 0) located at the center of the gap were used for measurement of magnetic field strengths. Magnetic field measurements were carried out with the magnetic probe hold

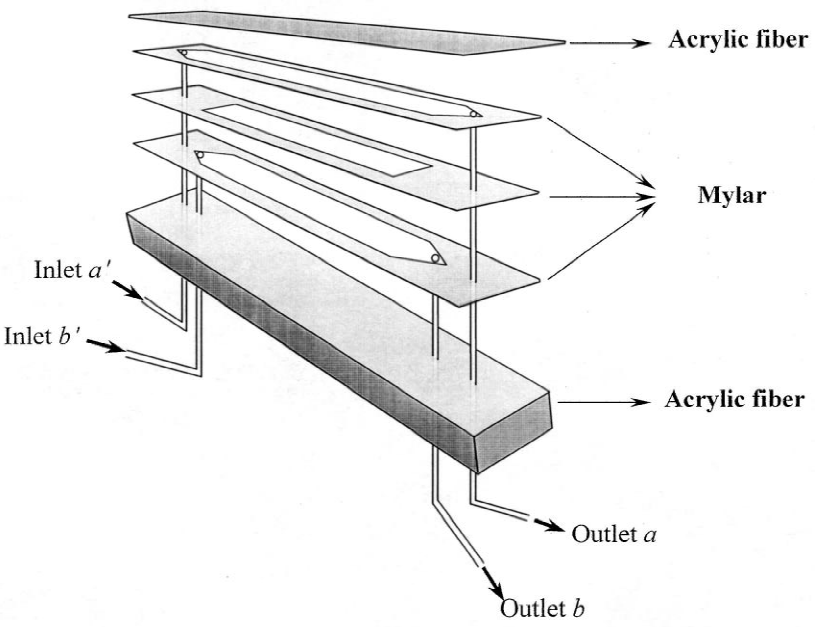

Fig. 3. Components of the magnetic SPLITT separator. Two inlets, inlet a′ and inlet b′, and two outlets, outlet a and outlet b, are shown. The edges of the centered mylar were used as inlet and outlet splitters.

in microscale adjustable stages for sensitivity of magnetic fields close to the gap center. Magnetic fields inside the channel were assumed to be equal to experimental measured values in the same distance from the gap center. The combined magnets and pole pieces measured 17.5×10×6.0 cm and weighted 5.5 kg. The distance between channel and magnetic gap was optimized for different flow-rates and accommodated particles with differing magnetic susceptibilities.

An LC pump (SSI series II, State College, PA), and micro tubing pumps (Eyela Mp-3, Rikakikai, Tokyo, Japan) were used to deliver samples and carriers into the separation channels; light microscopy (Olympus BX-50, Tokyo, Japan) was used for particles verification; a hemacytometer (a cell counting chamber with microscalar grids and fixed volumes) was used to count particles and calculate particle concentration. Silica particles (1–10 μm), molybdenum particles (<5 μm), and iron nitrate were purchased from Sigma Chemical (St. Louis, MO). Erbium chloride was obtained from Strem Chemicals (Newburyport, MA). M-450 dynabeads of 4.5 μm in diameter were obtained from Dynal®, (Lake Success, NY). Glass beads with sizes of 1–5 μm and polystyrene beads with size of 5 μm were obtained from Duke Scientific (Palo Alto, CA). Copper (II) oxide (<5 μm), chromium (III) oxide (<1 μm), tungsten (IV) sulfide (<2 μm), and iron (III) oxide (<5 μm) particles were obtained from Aldrich Chemicals (St. Louis, MO).

The carrier composition used for all particle experiments was 0.10 M carbonate buffer with pH equal to 6.0. Labeled silica particles were prepared using opposite charge attraction between positively charged ions and negatively charged silica surfaces. They were mixed, incubated for 60 min, and then washed with pH 6.0 carbonate buffer three times before use. Ion-labeled silica particles were purified before experimental use by removing particles not well-labeled via the SPLITT channel. The experimental conditions for this purification were $\dot{V}(a') = 3.6$, $\dot{V}(b') = 1.2$, $\dot{V}(a) = 2.4$, $\dot{V}(b) = 2.4$ ml min^{-1}.

Red blood cell labeling: Fresh blood cells from hospital were centrifuged at 50 *g* for 5 min to remove plasma. Then cells were washed with phosphate buffered solution (PBS) and centrifuged three

times before labeling. For labeling, 9 ml blood cells in PBS with 1 ml labeling ion solutions were mixed. The mixed solutions were incubated in ice for 60 min and shaken every 15 min. Solutions were centrifuged and washed with PBS three times to remove unreactive ions after incubation. Dye exclusion test was carried out with trypan blue stain and hemacytometer. The method was based on that viable cells did not take up dyes, whereas nonviable cells did. In viability test, 0.5 ml cell suspension was mixed thoroughly with 0.5 ml of 0.4% (w/v) trypan blue solution for 5 min before counting.

The fractional retrieval at outlet a (Fa) was calculated using the following equation:

$$Fa = \frac{N_a}{N_a + N_b} \quad (10)$$

where N_a was the number of silica particles exiting at outlet a, and N_b was the number of silica particles exiting at outlet b. The recovery percentage of labeled silica particles was calculated by adding the total number of labeled silica particles exiting at outlets a and b, and dividing by the total number of labeled silica particles entering at the inlets. At least 300 cells were counted in each of retrieval experiments. Pulsed sample injection meant injecting sample with a fixed volume of sample loop. Pulsed sample injection with a loop volume of 0.5 ml was used in the experiments of recovery and fractional retrieval.

Magnetic susceptibility measurement was done with an MPMS5 model superconducting quantum interference device (SQUID) magnetometer from Quantum Design (San Diego, CA USA). The cgs system and volume magnetic susceptibility, χ, were used throughout this study unless otherwise indicated.

4. Results and discussions

The first part of this study characterized the magnetic SPLITT system, second part developed preparative separation of magnetically susceptible particles. For system characterization, we emphasized the parallel mode since perpendicular-mode operation was examined in an earlier study [11].

Iron- and erbium-labeled silica particles were shown to be completely separated from glass beads, polystyrene latexes, and unlabeled silica particles in perpendicular-mode operation [11]. Copper-, iron- and erbium-labeled yeasts were successfully separated from unlabeled yeasts at various flow-rates in perpendicular-mode operation, as shown in Table 1.

Table 1
Fractional retrieval of ion-labeled yeasts at outlet a (Fa) in perpendicular-mode operation[a]

Sample	Inlet concentration (number/ml)	Inlet flow-rate (ml min^{-1})		Outlet flow-rate (ml min^{-1})		Fa (%)
		$\dot{V}(a')$	$\dot{V}(b')$	$\dot{V}(a)$	$\dot{V}(b)$	
Yeasts labeled with Er^{3+}	1.10×10^6	1.2[a]	0.4	0.8	0.8	100
		2.4[b]	0.8	1.6	1.6	100
		3.6[c]	1.2	2.4	2.4	100
Yeasts labeled with Fe^{3+}	1.10×10^6	1.2[d]	0.4	0.8	0.8	100
		2.4[e]	0.8	1.6	1.6	100
		3.6[f]	1.2	2.4	2.4	100
Yeasts labeled with Cu^{2+}	1.10×10^6	1.2[g]	0.4	0.8	0.8	100
		2.4[h]	0.8	1.6	1.6	100
		3.6[i]	1.2	2.4	2.4	100
Yeasts	1.10×10^6	1.2[a]	0.4	0.8	0.8	0
		2.4[b]	0.8	1.6	1.6	0
		3.6[c]	1.2	2.4	2.4	0

[a] Distances between channel and magnetic gap: a, 1.60 mm; b, 0.95 mm; c, 0.45 mm; d, 1.50 mm; e, 0.80 mm; f, 0.35 mm; g, 1.30 mm; h, 0.48 mm; i, 0.15 mm.

Table 2
Fractional retrieval of unlabeled and ion-labeled red blood cells (RBC) at outlet a (*Fa*) in perpendicular-mode operation[a]

Sample	Inlet concentration (number/ml)	Inlet flow-rate (ml min^{-1})		Outlet flow-rate (ml min^{-1})		*Fa* (%)
		$\dot{V}(a')$	$\dot{V}(b')$	$\dot{V}(a)$	$\dot{V}(b)$	
RBC labeled with Er^{3+}	1.28×10^6	1.2[a]	0.4	0.8	0.8	100
		2.4[b]	0.8	1.6	1.6	100
		3.6[c]	1.2	2.4	2.4	100
RBC labeled with Fe^{3+}	1.28×10^6	1.2[d]	0.4	0.8	0.8	100
		2.4[e]	0.8	1.6	1.6	100
		3.6[f]	1.2	2.4	2.4	100
RBC	1.28×10^6	1.2[d]	0.4	0.8	0.8	0
		2.4[e]	0.8	1.6	1.6	0
		3.6[f]	1.2	2.4	2.4	0

[a] Distances between channel and magnetic gap: a, 2.45 mm; b, 1.10 mm; c, 0.55 mm; d, 2.25 mm; e, 1.00 mm; f, 0.40 mm.

Iron- and erbium-labeled red blood cells were also successfully separated from unlabeled ones, as shown in Table 2.

Ions-labeled silica particles were also separated from unlabeled silica particles in parallel-mode operation, as shown in Table 3. The distance between channel and magnetic gap is greater in parallel-mode operation than perpendicular-mode operation. The distance differences are due to the gravity counteracts the magnetic forces for separation in perpendicular-mode operation. Several magnetically susceptible particles can also be separated from unlabeled silica particles in this study, as shown in Table 4. Chromium oxide particles are smaller and have lower susceptibilities than other particles, so they could only be completely separated at low flow-rate not at high flow-rates in our experiments.

We also tested parallel-mode retrieval (*Fa*) with particles and ion-labeled particles of varying carrier magnetic susceptibilities, as shown in Table 5. Retrieval from incomplete separation was intentionally chosen for better comparison. Particle and

Table 3
Fractional retrieval of ion-labeled silicas at outlet a (*Fa*) in parallel-mode operation[a]

Sample	Inlet concentration (number/ml)	Inlet flow-rate (ml min^{-1})		Outlet flow-rate (ml min^{-1})		*Fa* (%)
		$\dot{V}(a')$	$\dot{V}(b')$	$\dot{V}(a)$	$\dot{V}(b)$	
SiO_2 [a]	1×10^6	1.2	0.4	0.8	0.8	0
SiO_2 [b]		2.4	0.8	1.6	1.6	0
SiO_2 [c]		3.6	1.2	2.4	2.4	0
SiO_2 [a] labeled with Cu^{2+}	1×10^6	1.2	0.4	0.8	0.8	100
SiO_2 [b] labeled with Cu^{2+}		2.4	0.8	1.6	1.6	100
SiO_2 [c] labeled with Cu^{2+}		3.6	1.2	2.4	2.4	100
SiO_2 [d] labeled with Fe^{3+}	1×10^6	1.2	0.4	0.8	0.8	100
SiO_2 [e] labeled with Fe^{3+}		2.4	0.8	1.6	1.6	100
SiO_2 [f] labeled with Fe^{3+}		3.6	1.2	2.4	2.4	100
SiO_2 [g] labeled with Er^{3+}	1×10^6	1.2	0.4	0.8	0.8	100
SiO_2 [h] labeled with Er^{3+}		2.4	0.8	1.6	1.6	100
SiO_2 [i] labeled with Er^{3+}		3.6	1.2	2.4	2.4	100

[a] Distances between channel and magnetic gap: a, 2.10 mm; b, 1.10 mm; c, 0.50 mm; d, 3.30 mm; e, 1.40 mm; f=0.80 mm; g, 3.55 mm; h, 1.60 mm; i, 0.90 mm; j, 4.00 mm.

Table 4
Fractional retrieval of particles at outlet a (*Fa*) in parallel-mode operation[a]

Sample	Inlet concentration (number/ml)	Inlet flow-rate (ml min^{-1})		Outlet flow-rate (ml min^{-1})		*Fa* (%)
		$\dot{V}(a')$	$\dot{V}(b')$	$\dot{V}(a)$	$\dot{V}(b)$	
SiO_2 [a]	1×10^6	1.0	0.6	0.8	0.8	0
SiO_2 [a]		2.4	0.8	1.6	1.6	0
SiO_2 [a]		3.6	1.2	2.4	2.4	0
Cr_2O_3 [a]	1×10^6	1.0	0.6	0.8	0.8	100
Cr_2O_3 [a]		2.4	0.8	1.6	1.6	69.5
Cr_2O_3 [a]		3.6	1.2	2.4	2.4	42.3
Fe_2O_3 [b]	1×10^6	1.0	0.6	0.8	0.8	100
Fe_2O_3 [c]		2.4	0.8	1.6	1.6	100
Fe_2O_3 [d]		3.6	1.2	2.4	2.4	100
Fe[e]	1×10^6	1.0	0.6	0.8	0.8	100
Fe[f]		2.4	0.8	1.6	1.6	100
Fe[g]		3.6	1.2	2.4	2.4	100

[a] Distances between channel and magnetic gap: a, 0.10 mm; b, 13.60 mm; c, 12.10 mm; d, 10.90 mm; e, 114.30 mm; f, 90.63 mm; g, 85.35 mm.

labeled-particle retrievals were clearly smaller when the magnetically susceptible carrier ($MnSO_4$ solution with a χ value of 4.77×10^{-6}) was used due to the reduced $\Delta\chi$ values (relative magnetic susceptibilities change between samples and carrier). Dynabeads had much larger χ values versus carrier than other particles, so the ($\Delta\chi$) value and thus retrieval, was not significantly affected. Molybdenum and copper (II) oxide particles have smaller χ values than other particles so the $\Delta\chi$ change was more pronounced.

In order to determine the efficiency of the separation system, we fixed the distance between channel

Table 5
Fractional retrieval of particles and labeled particles at outlet a (*Fa*) in carriers with different magnetic susceptibilities[a]

Sample	Inlet flow-rate (ml min^{-1})		Outlet flow-rate (ml min^{-1})		*Fa*±SD[b] (%)	*Fa*±SD in $MnSO_4$ solution[c] (%)
	$\dot{V}(a')$	$\dot{V}(b')$	$\dot{V}(a)$	$\dot{V}(b)$		
Mo	2.4[a]	0.8	1.6	1.6	20.2±0.9	5.07±0.03
CuO	2.4[a]	0.8	1.6	1.6	40.1±2.1	10.2±0.5
WS_2	2.4[a]	0.8	1.6	1.6	30.8±1.5	20.7±0.9
Cr_2O_3	2.4[a]	0.8	1.6	1.6	69.5±3.9	44.8±2.2
Fe_2O_3	2.4[b]	0.8	1.6	1.6	81.2±4.1	70.8±3.6
Dynabead	2.4[c]	0.8	1.6	1.6	65.4±2.1	63.1±1.9
SiO_2 labeled with Cu^{2+}	2.4[d]	0.8	1.6	1.6	20.9±1.1	9.50±0.50
SiO_2 labeled with Fe^{3+}	2.4[d]	0.8	1.6	1.6	28.0±1.5	18.9±0.8
SiO_2 labeled with Er^{3+}	2.4[d]	0.8	1.6	1.6	38.2±1.6	28.1±1.2
Yeast labeled with Cu^{2+}	2.4[e]	0.8	1.6	1.6	60.3±2.7	47.0±2.2
Yeast labeled with Fe^{3+}	2.4[e]	0.8	1.6	1.6	65.1±3.2	49.9±2.1
Yeast labeled with Er^{3+}	2.4[e]	0.8	1.6	1.6	75.1±2.9	59.8±2.4

[a] Distances between channel and magnetic gap: a, 0.10 mm; b, 13.60 mm; c, 40.10 mm; d, 4.00 mm; e, 1.60 mm.
[b] SD, standard deviation, $n=3$.
[c] Volume susceptibility of the $MnSO_4$ solution from SQUID measurement was 4.772×10^{-6}.

Table 6
Minimal labeling concentrations of various ions required for complete separation of labeled silica particles[a]

Sample	Sample total number	Inlet flow-rate (ml min^{-1})		Outlet flow-rate (ml min^{-1})		Ion labeled concentration (M)	χ (dimensionless, cgs) (10^{-6})	*Fa* (%)
		$\dot{V}(a')$	$\dot{V}(b')$	$\dot{V}(a)$	$\dot{V}(b)$			
Parallel mode								
SiO_2 labeled with Er^{3+}	2.5×10^9	1.2	0.4	0.8	0.8	0.01250	48.6	100
SiO_2 labeled with Fe^{3+}		1.2	0.4	0.8	0.8	0.01625	48.6	100
SiO_2 labeled with Cu^{2+}		1.2	0.4	0.8	0.8	0.02500	48.6	100
Perpendicular mode								
SiO_2 labeled with Er^{3+}	2.5×10^9	1.2	0.4	0.8	0.8	0.01375	59.1	100
SiO_2 labeled with Fe^{3+}		1.2	0.4	0.8	0.8	0.01875	59.1	100
SiO_2 labeled with Cu^{2+}		1.2	0.4	0.8	0.8	0.02750	59.1	100

[a] Distance between channel and magnetic gap was 0.1 mm.

and magnetic gap and progressively decreased the labeling ion concentration until the retrieval (*Fa*) was less than 100%. The results for minimal concentrations of various labeling ions that yielded complete separation in this study are shown in Table 6. The minimal concentration of labeling ions required for complete separation is on the order of 10^{-2} M. This is equivalent to 3.01×10^{18} ions used for labelings by taking 0.2 molar ions concentration with volume of 0.5 ml. This corresponds to 10^9 labeling ions per particle for complete separation since 2.5×10^9 particles were used for labeling. Erbium needed the lowest concentration among the ions to achieve complete separation. Both erbium and ferric ions have higher magnetic susceptibilities than copper ion so they need lower labeling concentration for complete separation. It is also clear from the table that the minimal concentration of labeling ions in parallel-mode operation is lower than that required in perpendicular-mode operation. The minimal concentrations of the same labeling ion with various particles and differing flow-rates are shown in Table 7. This table shows that silica particles needed lower ion concentrations than yeasts and cells for complete separation. The minimal concentration of labeling ions required for complete separation increased as the flow-rates increased.

We also tried to calculate particle magnetic susceptibilities with the magnetic SPLITT system. Combining Eqs. (4), (6) and (9) with experimental

Table 7
Minimal concentration of labeling ions required for complete separation of labeled particles in parallel-mode operation[a]

Sample	Sample total number	Inlet flow-rate (ml min^{-1})		Outlet flow-rate (ml min^{-1})		Ion labeled concentration (M)	χ (dimensionless, cgs) (10^{-6})	*Fa* (%)
		$\dot{V}(a')$	$\dot{V}(b')$	$\dot{V}(a)$	$\dot{V}(b)$			
[a]SiO_2 labeled with Fe^{3+}	2.5×10^9	1.2	0.4	0.8	0.8	0.01625	48.6	100
		2.4	0.8	1.6	1.6	0.02375	97.2	100
		3.6	1.2	2.4	2.4	0.03000	145	100
[b]Yeast labeled with Fe^{3+}	2.5×10^9	1.2	0.4	0.8	0.8	0.04000	27.3	100
		2.4	0.8	1.6	1.6	0.04375	54.7	100
		3.6	1.2	2.4	2.4	0.02750	82.0	100
[c]RBC labeled with Fe^{3+}	2.5×10^9	1.2	0.4	0.8	0.8	0.04125	17.5	100
		2.4	0.8	1.6	1.6	0.04625	35.0	100
		3.6	1.2	2.4	2.4	0.05000	52.5	100

[a] Distance between channel and magnetic gap was 0.1 mm. Sample diameters: a, 3.0×10^{-4} cm; b, 4.0×10^{-4} cm; c, 5.0×10^{-4} cm.

Table 8
Measured magnetic susceptibilities of Dynabeads using the magnetic SPLITT fractionation system[a]

Sample	Inlet flow-rate (ml min^{-1})		Outlet flow-rate (ml min^{-1})		*Fa* (%)	Measured $\Delta\chi$ value (dimensionless, cgs)	Average of $\Delta\chi$ (dimensionless, cgs)	RSD (%)
	$\dot{V}(a')$	$\dot{V}(b')$	$\dot{V}(a)$	$\dot{V}(b)$				
Dynabeads (Parallel mode)	3.6[a]	1.2	2.4	2.4	70.0	0.0648	0.0651	2.06
	2.4[b]	0.8	1.6	1.6	65.4	0.0639		
	1.2[c]	0.4	0.8	0.8	66.8	0.0666		
Dynabeads (Perpendicular mode)	3.6[d]	1.2	2.4	2.4	45.5	0.0654	0.0637	2.21
	2.4[e]	0.8	1.6	1.6	54.3	0.0627		
	1.2[f]	0.4	0.8	0.8	90.3	0.0631		

[a] Distances between channel and magnetic gap: a, 35.10 mm; b, 40.10 mm; c, 50.10 mm; d, 36.10 mm; e, 39.40 mm; f, 45.00 mm.

retrieval, we can calculated the $\Delta\chi$ value for known drops in magnetic field strength obtained by experimental measurement. The results of calculated magnetic susceptibility for Dynabeads are shown in Table 8. These results are very consistent (approximately 2% variation) for parallel- and perpendicular-mode operation at various flow-rates. Most parts of the consistency came from the uniform Dynabeads size. This indicates that the theory works very well for both modes. The calculated value of Dynabeads magnetic susceptibility obtained using SQUID was 0.6232, very close to our measurements. The agreement of the calculated magnetic susceptibility from the SPLITT experiments with that from the well-established SQUID technique demonstrates that a simple theoretical treatment of the magnetic SPLITT technique is quite accurate. This further suggests that the magnetic SPLITT system can be accurately modeled using magnetic susceptibilities determined by other techniques.

Ion-labeled yeasts and ion-labeled red blood cells were also completely separated from unlabeled ones in parallel-mode operation, as shown in Tables 9 and 10. The separation distance between channel and magnetic gap required for success with ion-labeled yeasts and red blood cells is greater in parallel-mode

Table 9
Fractional retrieval of ion-labeled yeasts at outlet a (*Fa*) in parallel-mode operation[a]

Sample	Inlet concentration (number/ml)	Inlet flow-rate (ml min^{-1})		Outlet flow-rate (ml min^{-1})		*Fa* (%)
		$\dot{V}(a')$	$\dot{V}(b')$	$\dot{V}(a)$	$\dot{V}(b)$	
Yeasts labeled with Er^{3+}	1.10×10^6	1.2[a]	0.4	0.8	0.8	100
		2.4[b]	0.8	1.6	1.6	100
		3.6[c]	1.2	2.4	2.4	100
Yeasts labeled with Fe^{3+}	1.10×10^6	1.2[d]	0.4	0.8	0.8	100
		2.4[e]	0.8	1.6	1.6	100
		3.6[f]	1.2	2.4	2.4	100
Yeasts labeled with Cu^{2+}	1.10×10^6	1.2[g]	0.4	0.8	0.8	100
		2.4[h]	0.8	1.6	1.6	100
		3.6[i]	1.2	2.4	2.4	100
Yeasts	1.10×10^6	1.2[a]	0.4	0.8	0.8	0
		2.4[b]	0.8	1.6	1.6	0
		3.6[c]	1.2	2.4	2.4	0

[a] Distances between channel and magnetic gap: a, 0.80 mm; b, 1.10 mm; c, 50 mm; d, 1.65 mm; e, 0.90 mm; f, 0.40 mm; g, 1.45 mm; h, 0.55 mm; i, 0.2 mm.

Table 10
Fractional retrieval of unlabeled and ion-labeled red blood cells (RBC) at outlet a (*Fa*) in parallel-mode operation[a]

Sample	Inlet concentration (number/ml)	Inlet flow-rate (ml min^{-1})		Outlet flow-rate (ml min^{-1})		*Fa* (%)
		$\dot{V}(a')$	$\dot{V}(b')$	$\dot{V}(a)$	$\dot{V}(b)$	
RBC labeled with Er^{3+}	1.28×10^6	1.2[a]	0.4	0.8	0.8	100
		2.4[b]	0.8	1.6	1.6	100
		3.6[c]	1.2	2.4	2.4	100
RBC labeled with Fe^{3+}	1.28×10^6	1.2[d]	0.4	0.8	0.8	100
		2.4[e]	0.8	1.6	1.6	100
		3.6[f]	1.2	2.4	2.4	100
RBC	1.28×10^6	1.2[d]	0.4	0.8	0.8	0
		2.4[e]	0.8	1.6	1.6	0
		3.6[f]	1.2	2.4	2.4	0

[a] Optimized distances between channel and magnetic gap: a, 2.60 mm; b, 1.25 mm; c, 0.58 mm; d, 2.39 mm; e, 1.12 mm; f, 0.49 mm.

operation than in perpendicular-mode operation. This is because gravity acting on magnetically susceptible particles counteracts applied magnetic force during separation. The parallel mode separates magnetically susceptible particles with high densities and/or large diameters better than the perpendicular mode, because gravity acting on the magnetically susceptible particles tends to counteract the applied magnetic forces in perpendicular-mode operation. The distance difference between parallel- and perpendicular-mode operation became smaller as the flow-rate was increased. Preparative separation of ion-labeled yeasts and ion-labeled red blood cells were successfully separated from unlabeled ones. The viabilities of ion-labeled red blood cells after SPLITT fractionation were all above 97%, as determined by dye exclusion testing. This suggests that magnetic SPLITT fractionation has a good potential for biological applications like blood cell separation. Higher sample concentrations were also tested for complete separation in the magnetic SPLITT system. Convection from hydrodynamic particle coupling could cause sample overloadings and set the upper concentration limitations [6,14]. Field shielding could also play some roles in overloadings. The optimized result was 1.20×10^7 particles/ml using present setup. This corresponds to 7.20×10^8 particles/h in this study.

The limitations of magnetic SF are that SF is a binary separation process and SF is applicable to magnetically susceptible particles. A series array of SPLITT cells with different flow-rate and field setups along the main flow axis can be added to improve binary separation. At present SF works on the particles with $\Delta\chi$ larger than 1.75×10^{-5} [cgs]. Using electromagnet would increase magnetic field strength several times to extend magnetic SF applications to lower magnetically susceptible particles. Also electromagnet would make field strength adjustment easier than permanent magnets but at much higher cost.

5. Conclusions

We characterized magnetic SPLITT fractionation using parallel- and perpendicular-mode operation in this study. The parallel mode proved to be better than the perpendicular mode for separation of magnetically susceptible particles with high densities and/or large diameters, because gravitational forces acting on magnetically susceptible particles tended to counteract their own magnetic forces in perpendicular-mode operation. The minimal difference of magnetic susceptibility ($\Delta\chi$) for successful separation was found to be about 1.75×10^{-5} [cgs]. The minimal concentration of labeling ions required for complete separation was found to be about 10^9 labeling ions per particle in this study. The system showed good potential for simple measurements of particle magnetic susceptibilities. The system throughput was about 7.20×10^8 particles/h in this

study. Ion-labeled blood cells were found to be viable (>97%) after magnetic SPLITT fractionation. Magnetic SPLITT fractionation should become a useful separation technique for magnetically susceptible particles.

Acknowledgements

This work was supported by the National Science Council of Taiwan (NSC-87-2113-M-324-006).

References

[1] J.C. Giddings, Sep. Sci. Technol. 20 (1985) 749.
[2] S.R. Springston, M.N. Myers, J.C. Giddings, Anal. Chem. 59 (1987) 344.
[3] C.B. Fuh, M.N. Myers, J.C. Giddings, Ind. Eng. Chem. Res. 33 (1994) 355.
[4] J.C. Giddings, Sep. Sci. Technol. 23 (1988) 119.
[5] C.B. Fuh, J.C. Giddings, Sep. Sci. Technol. 32 (1997) 2945.
[6] C.B. Fuh, J.C. Giddings, Biotechnol. Progress 11 (1995) 14.
[7] C.B. Fuh, J.C. Giddings, J. Microcolumn Sep. 9 (1997) 205.
[8] C.B. Fuh, M.N. Myers, J.C. Giddings, Anal. Chem. 64 (1992) 3125.
[9] C.B. Fuh, S. Levins, J.C. Giddings, Anal. Biochem. 208 (1993) 80.
[10] R.G. Keil, E. Tsamakis, C.B. Fuh, J.C. Giddings, J.I. Hedges, Geochimica et Cosmochimica Acta 58 (1994) 879.
[11] S. Levin, G. Tawil, Anal. Chem. 65 (1993) 2254.
[12] C.B. Fuh, S. Chen, J. Chromatogr. A 813 (1998) 313.
[13] T.M. Vickrey, J.A. Gacia-Ramirez, Sep. Sci. Technol. 15 (1980) 1297.
[14] P.S. Williams, S. Levin, T. Lenczycki, J.C. Giddings, Ind. Eng. Chem. Res. 31 (1992) 2172.